"Gheorghe Asachi" Technical University of Iasi, Romania

ASSESSMENT OF CORROSION INHIBITORY EFFECT OF *Ruta chalepensis* FLAVONOID EXTRACTS ON *API 5L X52* STEEL IN 1M HCL MEDIUM

Meryem Amal Benghalia[1,2], Chahinez Fares[2], Abdelkader Khadraoui[3], Mohammed Hadj Meliani[2,4], Rami K. Suleiman[5]*, Ahmad A. Sorour[5], Ihor M. Dmytrakh[6], Zitouni Azari[4]

[1]*Laboratory for Water & Environment, Faculty of Technology, Hassiba Benbouali University of Chlef, B.P. 151, 02000 Chlef, Algeria*
[2]*Laboratory for Theoretical Physics and Material Physics, Hassiba Benbouali University of Chlef, B.P. 151, 02000 Chlef, Algeria*
[3]*Laboratoire de la valorisation des substances naturelles, Université Djilali Bounaama, Khemis-miliana, Algérie*
[4]*Laboratory LEM3, UMR CNRS 7239, 1 road d'Ars Laquenexy, CS 65820, 57078 Metz, France*
[5]*Center of Research Excellence in Corrosion, King Fahd University of Petroleum & Minerals (KFUPM), Dhahran 31261, Saudi Arabia*
[6]*Karpenko Physico-Mechanical Institute of National Academy of Sciences of Ukraine, 5 Naukova Street, 79060 Lviv, Ukraine*

Abstract

The development of green eco-friendly inhibitors for the corrosion of metallic surfaces in acid media is still considered as a major challenge and target for corrosion-mitigation engineers. We have prepared in this work 4 different extracts from the plant *Ruta Chalepensis* using methanol, chloroform, ethyl acetate, and aqueous ethyl acetate solvent systems. The flavonoids content, as well as the other oxygenated compounds, in the 4 extracts was carefully screened using the gas chromatographic–mass spectrometry (*GC-MS*) technique. The corrosion inhibition property of all extracts for *API 5L X52* steel in the hydrochloric acid medium has been carefully assessed using electrochemical techniques and surface-morphological characterizations. Our results revealed promising corrosion-inhibition properties for the methanol and chloroform extracts compared to other extracts and suggest potential applicability for the flavonoids from the studied plant as green corrosion inhibitors for steel substrates in acid media.

Key words: API 5L X52 steel, corrosion inhibitors, flavonoids, *Ruta Chalepensis*

Received: February, 2018; Revised final: February, 2018; Accepted: October, 2018; Published in final edited form: September, 2019

1. Introduction

The chemical, physical, and biological properties of plants make them candidate materials for the pharmaceutical and medical research (Farooqi et al., 1997; Houghton, 1995; Magufuli, 2009; Mukherjee et al., 1997; Mutasingwa, 2004; Philip et al., 2001). The antioxidants from natural sources can effectively inhibit food (Akbarirad et al., 2016; Cotea et al., 2018; Medini et al., 2014) and metal oxidation (Buchweishaija, 2009; Ndibe et al., 2018; Okafor et al., 2012; Onuegbu et al., 2013). Flavonoids are plants' secondary metabolites that are reported to have a promising interesting antioxidant activity (Brewer, 2011). Various studies have been conducted on the antioxidants properties of human diet and the reported results revealed that flavonoids can reduce the risk of several chronic human diseases, such as cardiovascular diseases, rheumatism, diabetes mellitus and cancer (Pong, 2003; Zhang et al., 2015)

* Author to whom all correspondence should be addressed: e-mail: ramismob@kfupm.edu.sa; Phone: +966-13-8607580; Fax: +966-13-8603996

via their ability to scavenge a wide range of reactive superoxide anion (O^-) oxygen species (Robak and Gryglewski, 1988; Takahama, 1985), hydroxyl radical (Husain et al., 1987) and peroxy radicals (Torel et al., 1986), as well as inhibitors of lipid peroxidation (Markesbery and Lovell, 1998; Williams et al., 2004) and as antimicrobial barriers (Cushnie and Lamb, 2005). However, the use of flavonoids as metal-oxidation inhibitors has not been much explored in the literature.

In this aspect, other studies reported that the corrosion of steel has been significantly inhibited using synthesized phenolic compounds, with π-electrons; aromatic rings and heteroatoms such as sulphur, nitrogen, and oxygen in their structure as corrosion inhibitors (Abdallah et al., 2012; Fouda et al., 2013; Vrsalovic et al., 2007, 2011). These compounds are part of a group of secondary metabolites in plants that can be distinguished as the flavonoic and non-flavonoic compounds.

Chemically, the flavonoids have a basic structure of diphenyl propane with 15-carbon atoms arranged in three rings (C_6-C_3-C_6), which are consisted (Fig. 1) of two phenyl rings (A and B) and heterocyclic ring (C). The level of oxidation and pattern of substitution of the C ring leads to various classes of flavonoids, whereas the difference in the pattern of substitution of the A and B rings determines the type of the individual compounds within a class (Brewer, 2011).

Flavonoids can be categorized into four major subgroups (i) chalcones, flavonoids having an open C ring, (ii) isoflavones are flavonoids in which B ring is linked to position 3, (iii) neoflavonoids correspond to flavonoids having the B ring linked to position 4, and (iv) flavones, flavonols, flavanones, flavanonols, flavanols or catechins, and anthocyanins refer to flavonoids where B ring is linked to position 2 (Brewer, 2011).
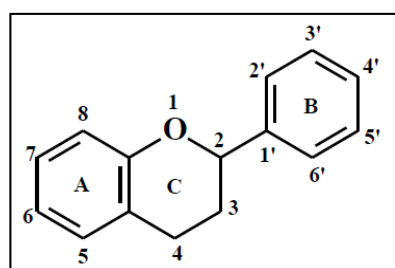

Fig. 1. Concept basic skeleton of flavonoids

Nowadays, the protection of metallic substrates against corrosion using eco-friendly (green) corrosion inhibitors is considered as a hot area of research. In our previous work, the inhibition efficiency of the leaves' extract of *Ruta chalepensis* (LERC) of API 5L X52 pipeline steel was studied in hydrochloric acid solution (1 M) at (308 K). LERC corrosion inhibitor can inhibit the partial reactions by decreasing the anodic metal dissolution and the cathodic hydrogen evolution reactions (mixed type). This behaviour can be attributed to the occurrence of a physical adsorption phenomenon of the active components of the plant extract on the steel surface (Benghalia et al., 2018).

Encouraged by the above, we aimed in this study to investigate the inhibition efficiency of the various classes of flavonoids. Our approach is to search for the appropriate class of flavonoids that can be extracted from the leaves of *Ruta Chalepensis* and prove to be able to serve as an effective corrosion inhibitor for the *API 5L X52* pipeline steel in 1M hydrochloric acid corrosive medium.

2. Experimental

2.1. Materials and the preparation of specimens

The corrosion inhibition effect of the developed inhibitors was studied on a low alloyed pipeline steel of grade *API 5L X52* (see Table 1 for the chemical composition), which is the most used steel grade in the existing Algerian gas pipelines network (Bouledroua et al., 2017; Elazzizi et al., 2015; Hadj Meliani et al., 2011a; Soudani et al., 2017).

The specimens were obtained and prepared from a pipe in service (Fig. 2). To prepare the steel surface for electrochemical experiments, it was pre-treated by grinding them with various emery silicon papers up to 1800 grade, rinsed with distilled water, degreased in ethanol, flushed repeatedly with bi-distilled water, and subjecting it finally to open-to-air room temperature drying. The exposed surface area of the steel specimen to the electrolyte was 0.25 cm² (Fig. 2).

2.2. Plant material and extraction

The fresh leaves of *Ruta chalepensis* were collected in the flowering period from Oued Fodda area (Chlef, North Algiers). The plant materials were cleaned by a proper successive washing with tap water followed by rinsing with bi-distilled water. Finally, the leaves were allowed to dry at room temperature for one week, grounded carefully into a fine powder, and then exposed to the extracting solvents.

The flavonoids were extracted using the extraction method described by Markham (Markham, 1982) with the modification proposed by Bruneton (Bruneton, 1993). The dried powder of *Ruta chalepensis* leaves (approximately 20 g) was macerated using a mixture of methanol (85%) and water 7:3 (v/v) for 72 hours accompanied by the renewal of solvent mixture every 24 hours. The mixture was filtered on filter paper No. 11 and the filtered aqueous extracts were subjected to evaporation at low pressure at 35°C using a rotavapor and stored at 4°C for 48 hours. The aqueous phase was washed three times with the same volume of *n*-hexane solution (v/v) to remove any residual proteins.

The resulting solution was mixed thoroughly with an equal volume of chloroform to extract the aglycone flavonoids. The residual aqueous phase was subjected to another liquid-liquid extraction using the ethyl acetate solvent.

Table 1. Chemical composition of the *API 5L X52* steel (in weight %) (Hadj Meliani et al., 2011b)

C	*Mn*	*P*	*Si*	*Cr*	*Ni*	*Mo*	*S*	*Cu*	*Ti*	*Nb*	*Al*	*Fe*
0.22	1.22	-	0.24	0.16	0.14	0.06	0.04	0.19	0.04	<0.05	032	Bal.
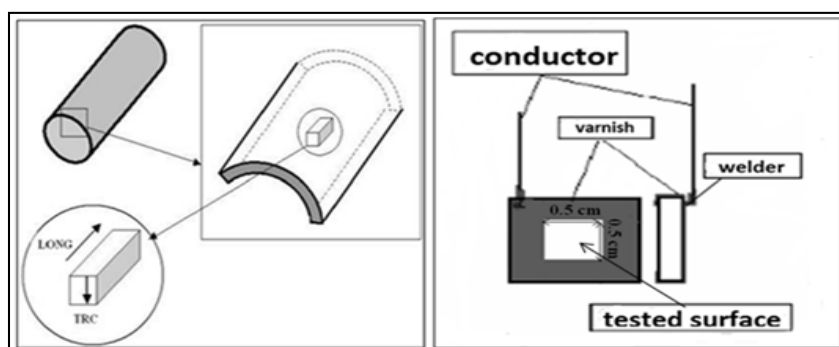
Fig. 2. Samples preparation: specimen's geometry and orientation regarding the initial pipeline and exposed surface area for electrochemical tests

The extraction was repeated 10 times and the aqueous and organic phases were separated following the same steps reported in the first extraction. All extracts were stored at a temperature of 4°C prior to using. Four fractions have resulted from the sequential extraction and the obtained extracts were denoted as per the solvent used for their separation as follows: methanol extract (*ME*), chloroform extract (*CE*), organic ethyl acetate extract (*OEAE*), and aqueous ethyl acetate extract (*AEAE*). The extraction yields were calculated using the procedure reported previously in the literature (Umoren et al., 2018).

2.3. Determination of total flavonoid content (TFC)

Total flavonoid content in each extract was determined using the aluminium chloride colorimetric method and using standard solutions at concentrations ranging from 0.005 to 0.125 mg/mL of catechin in 80% methanol (Bahorun et al., 1996). Firstly, 500 μL of each extract was diluted and mixed with 1500 μL of distilled water, 150 μL of nitrite sodium (5% $NaNO_2$), 150 μL aluminium chloride solution (10% $AlCl_3$) (m/v) and 500 μl of sodium hydroxide (4% *NaOH*). The mixture was mixed carefully and exposed to incubation at room temperature for 30 min. After incubation, the absorbance of the mixture was measured at 510 nm vs. a reagent blank containing water instead of the sample using a UV-visible spectrophotometer model LIBRA S6. The standard curve was constructed using catechin solution and the TFC was expressed in milligrams of catechin equivalent per gram of the dry extract (mg QE /g). All samples were analyzed in triplicate.

2.4. Antioxidant activity

Ferric Reducing Antioxidant Power (*FRAP*) method (Oyaizu, 1986) was applied to measure the antioxidant activity of the flavonoids extracts. This method is utilizing the potential antioxidant of the

flavonoids extracts to reduce the ferric-tripyridyltriazine (*Fe^{3+} TPTZ*, colourless) to a blue complex formation of the ferrous-tripyridyltriazine (*Fe^{2+} TPTZ*).

FRAP assay of the sample extract was conducted using the method described previously by Oyaizu (Oyaizu, 1986). The extract concentration that gave a 0.5 absorbance (IC50) was established from the absorbance at 700 nm versus extract concentration plot.

2.5. GC-MS and FTIR analysis

The identification of the natural compounds in each extract was made by the HP-6800 GC-MS instrument that is coupled to a mass spectrometer 5973 NMS. The ionization mode in the system was the electronic impact and the separation of compounds was achieved on column HP-5 type (5% phenyl methyl siloxane, 30 mm length, 0.25 mm internal diameter, and 0.25 μm film thickness). In the first step, the oven temperature programming was set at 70°C for 5 min then a temperature ramp of 10°C/min was applied to reach 220°C within 15 min of the test. In the second step, a ramp of 4°C/min was applied to reach a temperature of 280°C within 05 min. Pure helium was employed as a carrier gas with a flow rate of 0.5 mL/min and a 1 μL volume of the sample was manually injected into the system using a splitless injection mode. The FTIR characterization was carried out on the flavonoids extracts obtained from *Ruta chalepensis* Leaves. The equipment used was Varian 4100 Spectrum coupled to the UMA 600 microscopy. They were recorded within the wavenumber range of 4000-600 cm^{-1}.

2.6. Weight loss measurements

To find the corrosion rate (C_R) and inhibition efficiency (*Eg*), we have performed the gravimetric analysis. The tests were conducted using the standard

weight loss measurements and by immersing the specimens continuously in 1M *HCl* media with and without the flavonoids extract for 24 hours at 298 K. Calculations involved in these measurements can be found elsewhere (Obot et al., 2015).

2.7. Electrochemical measurements

The electrochemical tests were carried out using a PGP 201 Potentiostat with Volta Master 4 software and connected to a standard three-electrode cell. A large grid of platinum was used as a counter electrode (*CE*), whereas the saturated calomel electrode (*SCE*) and the steel specimen was acted as reference (*RE*) and working (*WE*) electrodes, respectively. The adopted procedure for the electrochemical measurement in our study was as follows: after immersing the specimen in the working corrosive medium with and without flavonoids extracts, the open circuit potential (*OCP*) was measured until its stabilization (about 1 hour). After that, the potentiodynamic polarization curves were obtained under the scan rate of 0.5 mV/s using a potential range of ±1000 mV from *OCP*. From these curves, the values of corrosion current density (i_{corr}) were determined for each test condition. The values of corrosion current density in the absence and presence of inhibitor in the corrosive medium were used to calculate the inhibition efficiency (EI$_{pol}$) as per the procedures described previously in the literature (Ndibe et al., 2018).

The EIS measurements were carried out using an AUTOLAB analyzer controlled by software NOVA 1.10 software. Impedance spectra were obtained in the frequency range of 100 KHz to 100 mHz and all potentials were reported versus SCE. A sine wave with 10 mV amplitude was used to perturb the system. The obtained impedance data were plotted and given in the Nyquist representation. The charge transfer resistance (R_t) values for the immersed samples in the absence and presence of the inhibitor were used to calculate the inhibition efficiency (E_{Rt}) (Umoren et al., 2018).

2.8. Surface characterization analysis

The immersed steel surfaces in 1M *HCl* medium (at 298 K for 24 h) loaded with or free from any flavonoids extract were morphologically analyzed using a scanning electron microscopy (SEM, Bruker Nano, Quantax) technique that is coupled with energy dispersive X-ray analysis (*EDX*) and Optical 3D surfaces measurement systems (Alicona's optical 3D).

3. Results and discussions

3.1. Screening of flavonoids content in the plant extracts

The evaporated methanol, chloroform, organic ethyl acetate and aqueous ethyl acetate extracts

obtained from 20 g of the plant material (*Ruta chalepensis*) were weighed and the extraction yields are shown in Fig. 3. The percentage yield of the extracts varied from 4.567 % to 1.087 %. The highest yield of the solid residue was obtained using methanol and chloroform as solvents in the extraction (Fig. 3).

The flavonoids contents in different extracts were expressed in mg catechin per g dry weight basis by comparison with catechin standard curve, and the flavonoids yield was calculated using the formula: Y = 1.05x +0.12 with R^2 = 0.992. The chloroform extract was found to contain the highest flavonoids content (about 80%) followed by the methanolic extract (Table 2).

3.2. Results of GC-MS and FTIR analysis

The identification of the individual organic compounds in the four extracts (ME, CE, OEAE, and AEAE) was achieved using a GC-MS system. Fig. 4, 5, 6, and 7 presented the GC-MS chromatograms of the flavonoids extracts: ME, CE, OEAE and AEAE, respectively.

Table 2. Total flavonoid content in extracts of *Ruta Chalepensis*

Extract	*mg of QE /g of extract*
Methanol	72 ± 0.375
Chloroform	80 ± 0.843
Organic ethyl acetate	41 ± 0.457
Aqueous ethyl acetate	22 ± 0.942

By analyzing the MS data of each peak in the chromatogram of ME (Fig. 4), we were able to identify 16 different compounds, which represent 94.65% of the total content. The majority of the identified compounds are furocoumarins having an acetone functional group such as methoxsalen (at a retention time of 24.43 min and a percentage of 52.28%), bergapten (24.79 min, 4.89%) and isopimpinellin (29.24 min, 2.48%). A flavonoid was detected at a retention time of 44.70 min and was identified as cirsimaritin (25.13%). The compound with a percentage of 5.21% and detected at a retention time of 40.89 min was identified as bis (2-Ethylhexyl) phthalate. This compound has a carbonate functional group.

In the *CE* (Fig. 5), compounds of various organic functionalities were identified, namely: alcohols (2-penten-1-ol 19.70%), acetone (4H-pyran-4-one 4.73%; 2,4-imidazolidinedione 1.08%; 2-oxepanone 0.51%; o-benzoquinone 0.68%; 2H-1-benzopyran-2-one 20.02%); amine (1-pyrrolidineethanamine 0.63%; isoxazolidine 0.59%; cuanozin 0.57%) and carboxylic acid as: heptanoic acid 14.907%; 5-aminovaleric acid 0.38%; hexadecanoic Acid 0.991%) and phenol as: 4-Vinyl-2-Methoxy-Phenol 1.5782%; and naphthalenol 6.46%. The *CE* contains the methoxsalen with a lower concentration (about 3.043%) than *ME*.
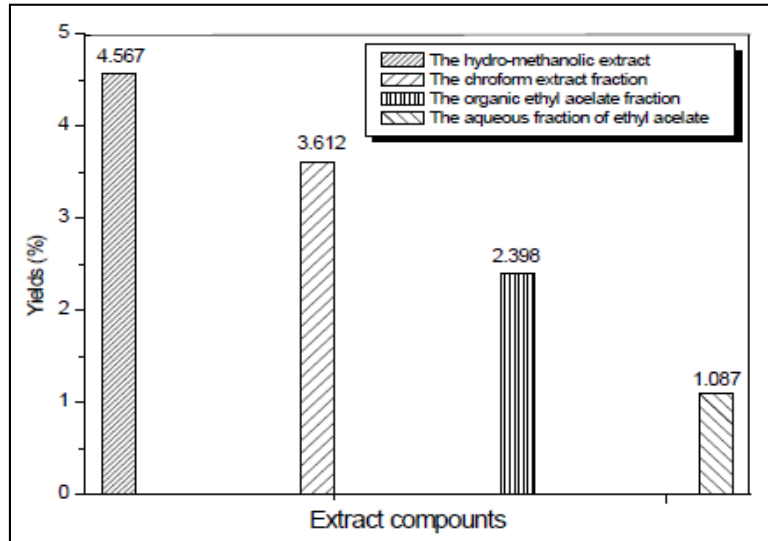
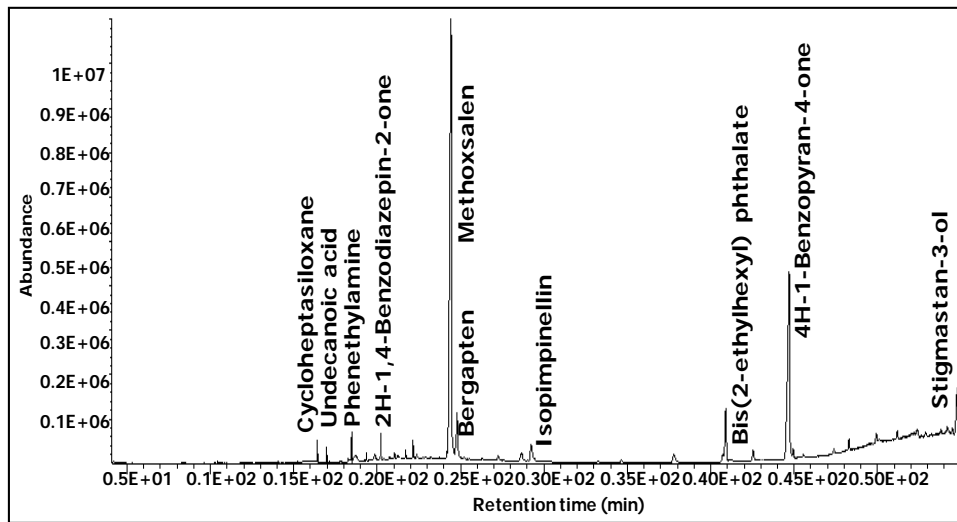**Fig. 3.** The yields of the dried solid residue after extracting a 20 g of dried plant leaves
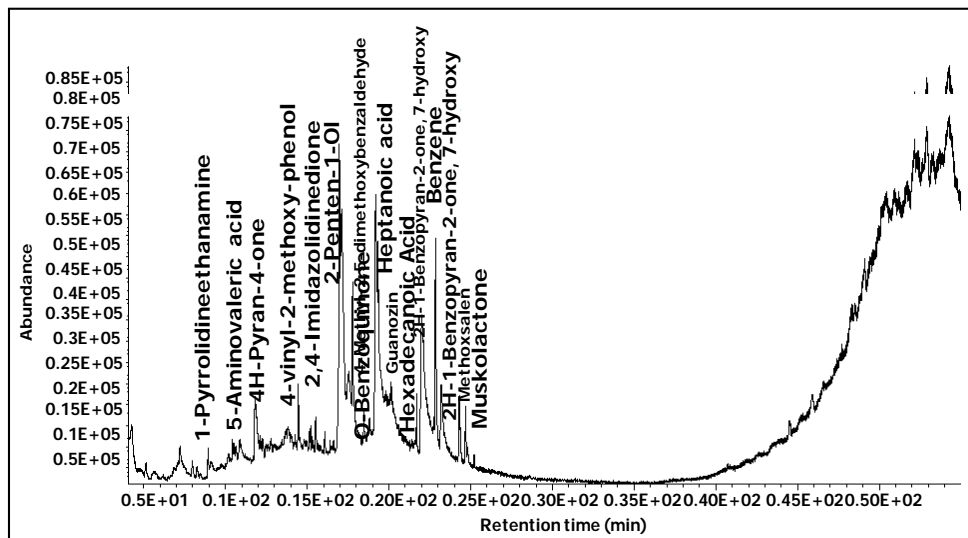

Fig. 4. GC-MS chromatogram of the *ME* extract

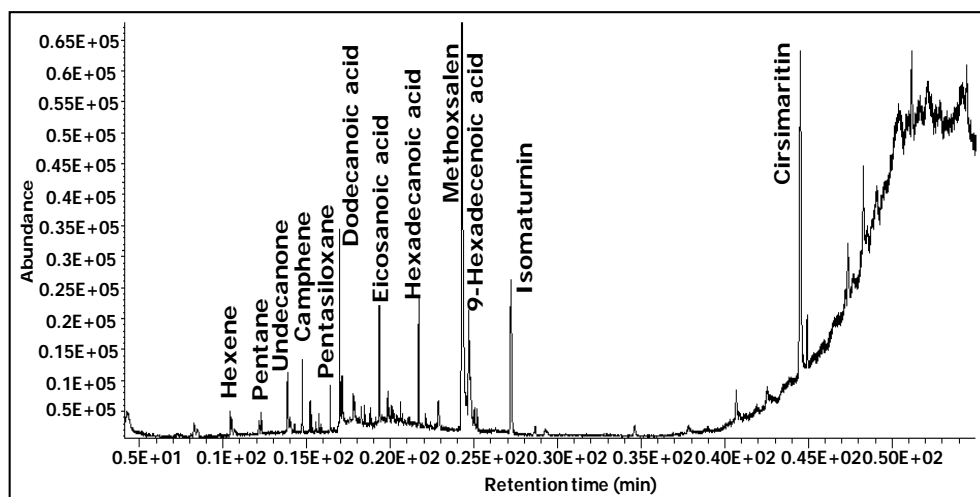

Fig. 5. GC-MS chromatogram of the *CE* extract
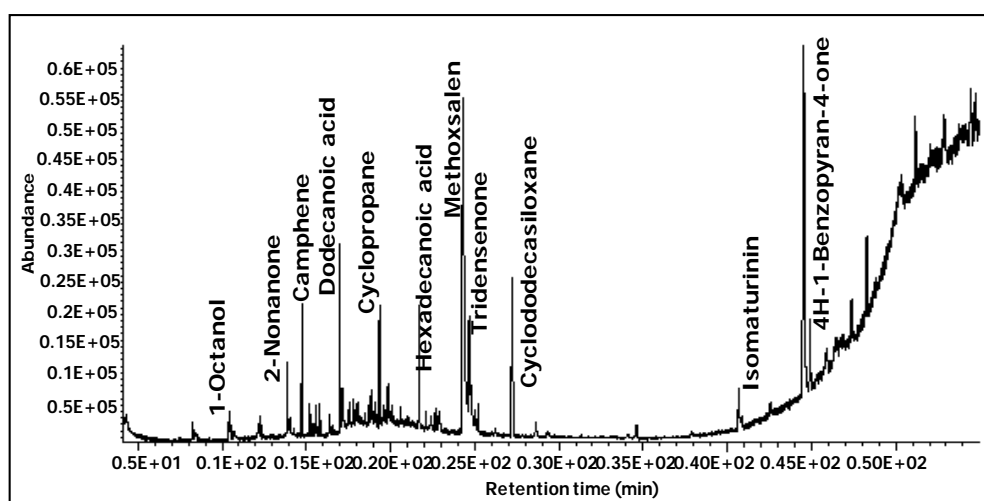
Fig. 6. GC-MS chromatogram of the *OEAE* extract

Fig. 7. GC-MS chromatogram of the *AEAE* extract

Table 3. *FTIR* Bands of flavonoids spectra obtained from *FTIR* Spectra

Bands / Extracts	υ O-H cm^{-1}	υ C-H cm^{-1}	υ C=O ester cm^{-1}	δ CH3 cm^{-1}	υ C-O cm^{-1}	υ C-O cm^{-1}	δ =C-H cm^{-1}
EM	3648, 3586, 3447, 3414, 3364, 3314	2832, 2503, 2926	1729	1440	-	1025	818
EC	3524, 3484, 3416, 3359, 3279, 3233	2829, 2522	-	1440	-	1013	-
OEAE	3630-3200	2930-2530	1847	1450	1117	1023	824
AEAE	3300-3480	2830-2820	1861	1460	1108	1017	815

The highest flavonoids content was obtained for the *CE*, but unfortunately, they were not detected by *GC-MS* as they might be deteriorated by the relatively high final temperature of the oven in *GC-MS*. In the *OEAE* and *AEAE* extracts (Figs. 6 and 7, respectively), we have also detected the presence of other compounds of beneficial functional groups for these compounds to function as corrosion inhibitors. The two peaks with the highest intensity observed in Figs. 4c and 4d were identified to contain the Methoxsalen compound with a percentage of 29.43% (*OEAE*) and 17.614% (*AEAE*), respectively. 4H-1-Benzopyran-4-one with a percentage of 21.49% and 15.89%, respectively was also found in the two chromatograms. These compounds contain oxygen as

a heteroatom in their chemical structure which makes them promising corrosion inhibitors.

The *FTIR* spectra of the four flavonoids extracts obtained from the *Ruta chalepensis* leaves were presented in Fig. 8. The characteristic bands obtained from spectra were listed in Table 3.

All extracts showed major IR peaks that are characteristic of flavonoids. The intense O-H stretch peaks observed between 3300-3284 cm^{-1} and the symmetric stretching vibrations of CH/CH$_2$ corresponding to glucoside groups between 2849-2853 cm^{-1} support the existence of polyphenols/flavonoids. Aromatic functionality is confirmed by the detected peaks between 1600 cm^{-1} and 1454 cm^{-1}. The stretching vibration of the

carbonyl functionality of aldehydes and ketones from triglycerides and polyphenols are observed at 1730 cm^{-1}, 1847 cm^{-1}, and 1861 cm^{-1}. The absorption bands at 1013 cm^{-1} and 1117 cm^{-1} are associated with the C-O stretching vibrations of ester, while the bands at 818 cm^{-1}, 815 cm^{-1}, and 824 cm^{-1} correspond to the in-plane deformation vibrations of C-H bond.

3.3. Evaluation of the antioxidant activity

The evaluation of the antioxidant activity of different flavonoid-rich extracts was attained using the *FRAP* method. The reduction capacity of these extracts to reduce the ions Fe^{3+} to Fe^{2+} was compared with the two known antioxidants ascorbic acid and *BHT* and the obtained results are depicted in Table 4.

It can be seen from the results reported in Table 3 that all extracts demonstrated a level of electron-donating capacity but to a different extent among the studied extracts. The electron-donating capacity of all extracts was in the following order: *CE > ME > AEAE > OEAE*. These results predict a promising ability for the flavonoids extracts, especially the chloroform and methanol extracts, to inhibit the rust formation ($Fe_2O_3.nH_2O$), i.e. reducing the corrosion of steel.

3.4. Weight loss measurements

The inhibition efficiency and corrosion rate obtained from the gravimetric measurements of API 5L X52 immersed in an acidic medium free from any inhibitor additive or having 0.5 g/L of the individual flavonoid-rich extracts are depicted in Table 5. The analysis of data reported in Table 5 reveals that the addition of all types of extracts of the plant *Ruta Chalepensis* decreases the weight loss of *API* steel *X52* in acidic medium. The inhibition efficiency reached a maximum of 80.65 % for the *ME*. Hence,

the inhibition efficiency of the various extracts can be ranked as: *ME > EC > AEAE > OEAE*.

Table 4. Antioxidant activities by *FRAP* assays for different extracts

Extracts	*FRAP*
Methanolic extract	0.321 nm
Chloroformic extract	0.605 nm
Organic ethyl acetate extract	0.113 nm
Aqueous ethyl acetate extract	0.209 nm
Ascorbic acid or *BHT*	2.284 nm
EC50 methanolic extract (mg/ml)	20
EC50 chloroformic extract (mg/ml)	15
EC50 organic ethyl acetate extract (mg/ml)	28
EC50 aqueous ethyl acetate extract (mg/ml)	25
EC50 ascorbic acid (mg/ml)	0.5

Table 5. Inhibition efficiency and corrosion rate of *API 5L X52* immersed in 1M *HCl*, in the absence and presence of 0.5g/L of one flavonoid extract at 298 K

Extract	*W(mg/cm².h)*	*Eg*
1 M HCl (Blank)	0.1548	-
1 M HCl + 0.5 g/L ME	0.0299	80.65
1 M HCl + 0.5 g/L CE	0.0475	69.32
1 M HCl + 0.5 g/L EAOE	0.0747	51.74
1 M HCl + 0.5 g/L EAEA	0.0675	56.39

3.5. Electrochemical evaluation

Potentiodynamic polarization curves for the immersed pipeline steel samples in 1M *HCl* solution in the absence/presence of various *Ruta chalepensis* extracts are shown in Fig. 9. The electrochemical parameters for the studied steel samples extracted from the Tafel plots of polarization curves are also available in Table 6 as corrosion potential E_{corr}, corrosion current density i_{corr}, and inhibitor efficiency EI_{pol} values.
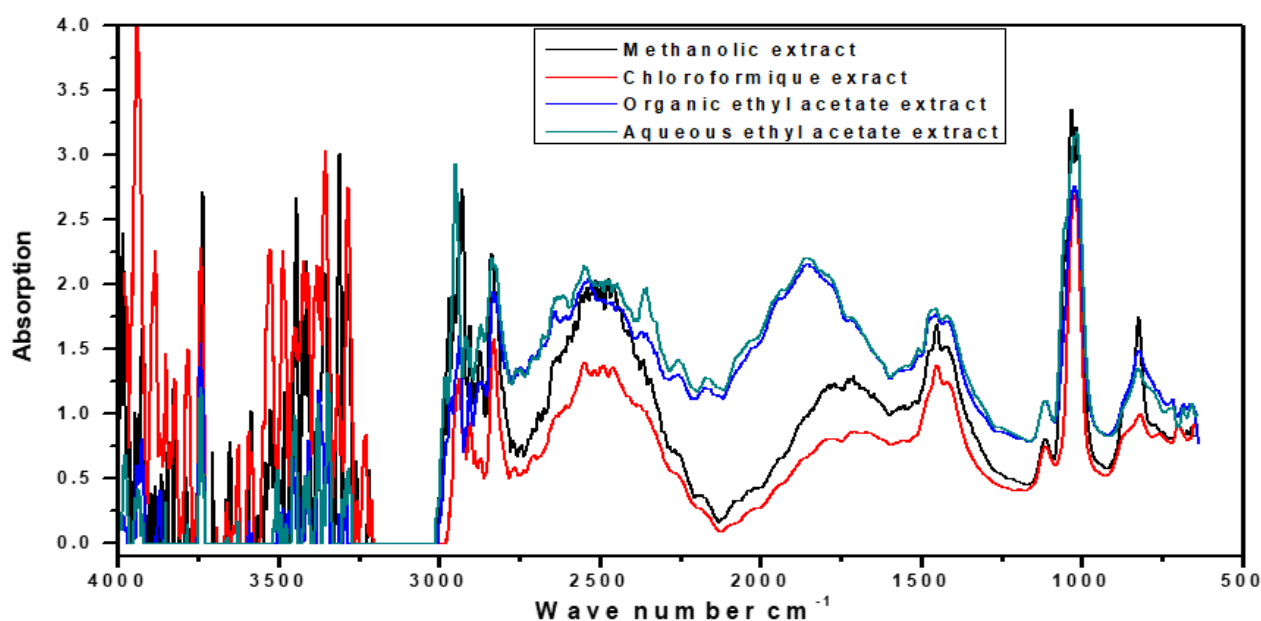

Fig. 8. *FTIR* Spectra of the various *Ruta chalepensis* extracts

It is clear from the results in Table 6 that the addition of *Ruta chalepensis* extract induced a high degree of corrosion inhibition property on the steel surfaces, as it can be proved from the EI_{pol} values of extract-loaded solutions (75.27% to 88.17%) comparing to the blank solution. The addition of the chloroform extract to the acidic medium (0.5 g/L) yielded the highest efficiency (about 88.17%) compared to the other extracts. The presence of inhibitors causes the shift of both cathodic and anodic branches of the polarization curves as compared with the blank solution. This indicates that the inhibitors can affect both the cathodic and anodic processes (Khadraoui et al., 2016). Furthermore, the presence of inhibitors does not induce a significant shift in the E_{corr} of the blank solution as can be seen from the polarization curves displayed in Fig. 9; thus, these inhibitors can be classified as a mixed-type inhibitor type.

Table 6. Electrochemical parameters of API 5L X52 steel in 1M HCl with and without the addition of various *Ruta chalepensis* extracts

	$-E_{corr}$ (mV)	i_{corr} (mA/cm²)	EI_{pol} (%)
1M HCl (Blank)	530	37.2	-
1M HCl + 0.5 g/L methanolic extract	607	7.2	80.65
1M HCl + 0.5 g/L chloroformic extract	487	4.4	88.17
1M HCl + 0.5 g/L organic ethyl acetate extract	633	6.8	81.72
1M HCl + 0.5 g/L aqueous ethyl acetate extract	576	9.2	75.27

Fig. 10 displayed the Nyquist diagrams of the steel samples exposed to 1M HCl in the absence and presence of individual flavonoids extract of the plant *Ruta chalpensis*. These diagrams are obtained after a 30-min immersion in an open circuit at room temperature. The impedance parameters deduced from the analysis of the Nyquist diagram and values of the inhibitor efficiency E_{Rt} are given in Table 7.

In the presence of the flavonoids extracts, Nyquist diagrams were depressed into the real axis and describe an unperfected semi-circle. The addition of the flavonoid-rich extracts did not alter the impedance profile indicating that the rate-determining step is the charge transfer process. The deviation from obtaining a perfect semicircle is due some inhomogeneity or surface roughness of the steel surface which is confirmed later by *SEM* and Optical *3D* characterizations.

The charge-transfer resistance (R_t) values can be calculated from the difference in the impedance values at lower and higher frequencies. Equation 1 below was used to compute the double-layer capacitance (C_{dl}).

$$C_{dl} = \varepsilon \varepsilon_0 \frac{A}{d} \tag{1}$$

where ε: the dielectric constant of the film, ε_0: vacuum permittivity (8.85 x 10⁻¹² F.cm⁻¹), A: active surface, and d: film thickness.

The increase in C_{dl}, might be resulted from the increase in the local dielectric constant or the decrease in the film thickness as per the Helmoltz assumption (Eq. 1). This evolution suggests that flavonoids extracts molecules act its function as corrosion inhibitors by an adsorption phenomenon at the metal solution/interface. As seen from Fig. 10, the diameter of the semicircle increases after the flavonoids extracts additions to the *HCl* media. This increase is more pronounced for the *ME* (67.11%).
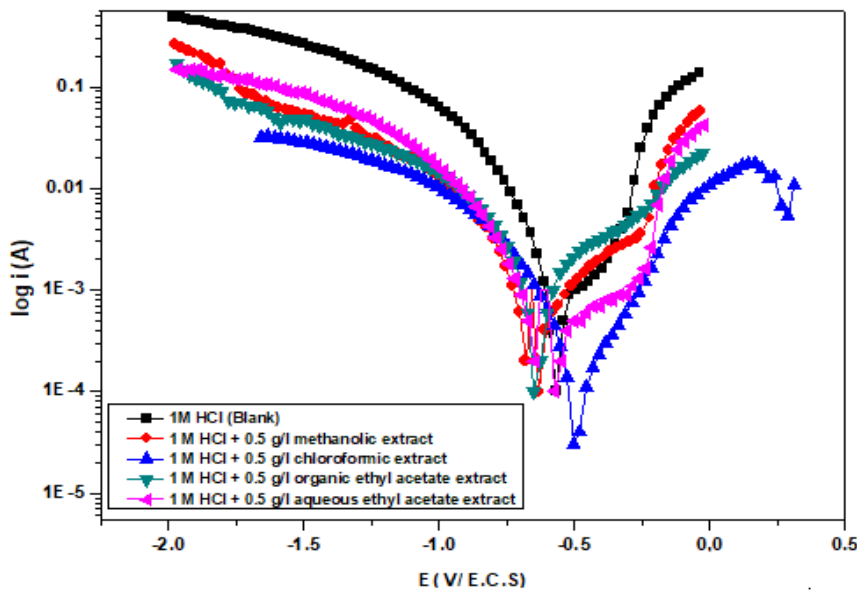

Fig. 9. Polarization curves of the API 5L X52 steel in 1M HCl in the absence and presence of different *Ruta chalepensis* extracts
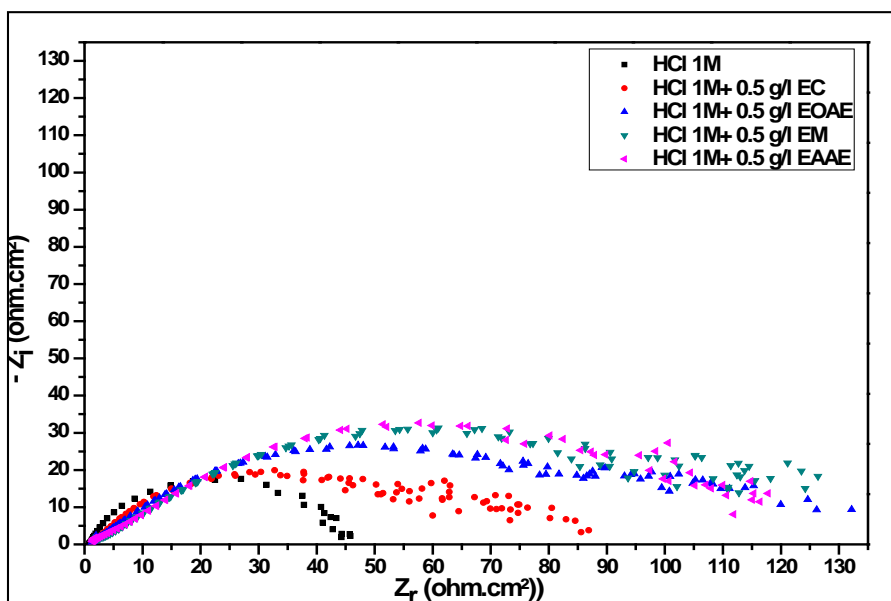
Fig. 10. Nyquist impedance plots for APIX52 in 1M HCl in the absence and presence of 0.5g/L of different *Ruta chalepensis* extracts

Table 7. Impedance parameters for corrosion of *API 5 LX52* in 1*M HCl* in the absence and presence of different of *Ruta chalepensis* extracts at 298 K

Extracts	*R_e*	*Rt(ohm.cm²)*	*F_{max} (Hz)*	*C_{dl} (µF.cm²)*	*E_{Rt}*
HCl 1M	0.84	45.16	6.87	513.25	-
HCl 1M+0.5 g/L ME	0.58	137.31	12.07	96.05	67.11
HCl 1M+0.5 g/L CE	0.68	132.25	5.18	232.35	65.85
HCl 1M+0.5 g/L OEAE	0.76	86.33	9.10	202.52	47.69
HCl 1M+0.5 g/L AEAE	0.70	127.47	6.87	181.83	64.57

3.6. Surface characterization analysis

3.6.1. SEM and EDX analysis

The scanning electron microscopy (*SEM*) images accompanied with the electron-dispersive X-ray spectroscopy (*EDX*) spectra on the whole surface of the studied pipeline steel specimens after immersion for 24 hours in *1M HCl* solutions free and containing an individual plant extract are shown in Figs. 11, 12,13, 14, 15, and 16, respectively.

The surface morphology of the raw pipeline steel contains some polishing scratches (Fig. 11). The *EDX* spectrum of this non-corroded sample showed peaks for Fe, Mn, Si elements. The absence of any peak corresponding to oxygen in this spectrum is evidence for the absence of any corrosion products on the surface of this sample. The *SEM* images of corroded surfaces after 24 h of immersion in the neat *1M HCl* solution can be seen in Fig. 12. The presence of a peak corresponding to oxygen in the *EDX* spectrum of this sample and the accumulation of corrosion products on its surface confirms the formation of oxides on the metal surface and thus, the occurrence of corrosion. The selective electrochemical dissolution of the alloyed components was also detected after 24 h of immersion in inhibitor-loaded *1M HCl*. The SEM images confirm (Fig. 13, 14, 15, and 16) that extracts inhibited significantly the corrosion of steel surfaces.

The images suggested relatively smooth steel surfaces for the samples immersed in *1M HCl* solution having 0.5 *g/L* of an individual extract compared to the images recorded for the inhibitor-free *HCl* medium (Fig. 12). These observations are more visible for the cases of the chloroform and methanol extracts (Fig. 13 and 14) which supports that these extracts promote the formation of a protective layer on the steel surface which ultimately inhibits the onset of corrosion processes.

The *EDX* spectra for both *CE* and *ME* extracts showed a significant decrease in the intensity of oxygen peak, which reveals a reduction in the formation of corrosion products on the surface of the studied pipeline steel. Overall, the *SEM* observations confirm the excellent inhibition efficiency of the *CE* comparing to other extracts. This indicates promising applicability for the *CE* as a corrosion inhibitor for *API 5L X52* steel in acidic media.

3.6.2. Optical 3D surface characterization

An optical profiler is a powerful tool for evaluating the surface properties especially the surface roughness. The two-dimensional and three-dimensional optical profiler images of the pipeline steel surface in the presence and absence of 0.5 g/L of various extracts in *1M HCl* are shown in Figs. 17 and 18, respectively.
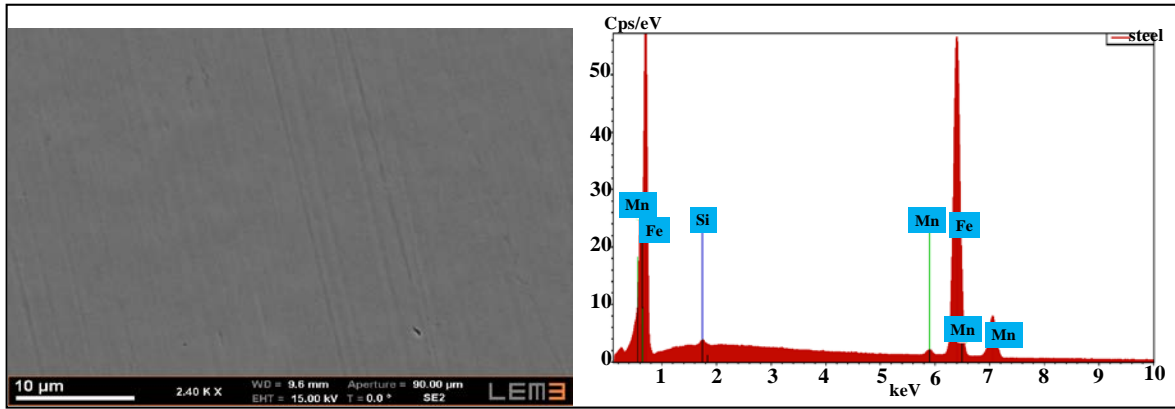
Fig. 11. Top-surface *SEM* image and *EDX* spectrum of the pipeline steel sample: a) without immersion in acidic medium
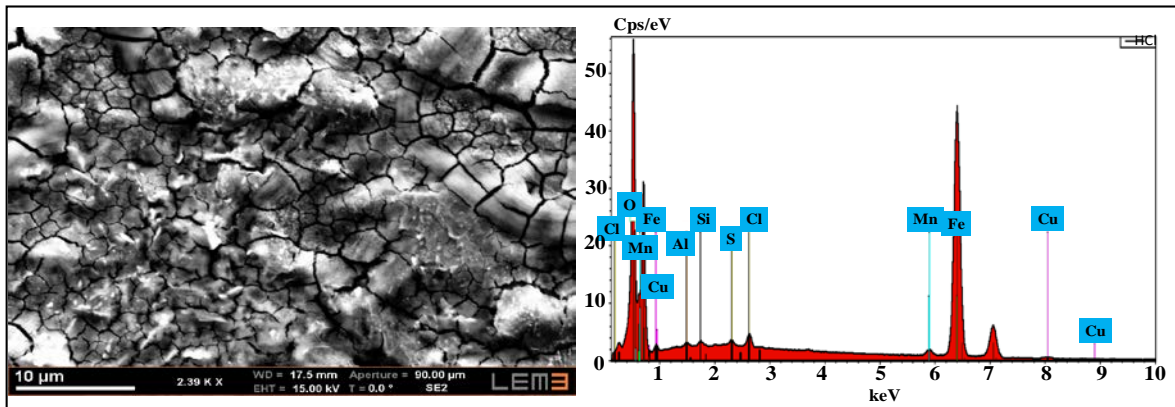

Fig. 12. Top-surface *SEM* image and *EDX* spectrum of the pipeline steel sample after 24 h of immersion in inhibitor-free *1M HCl*
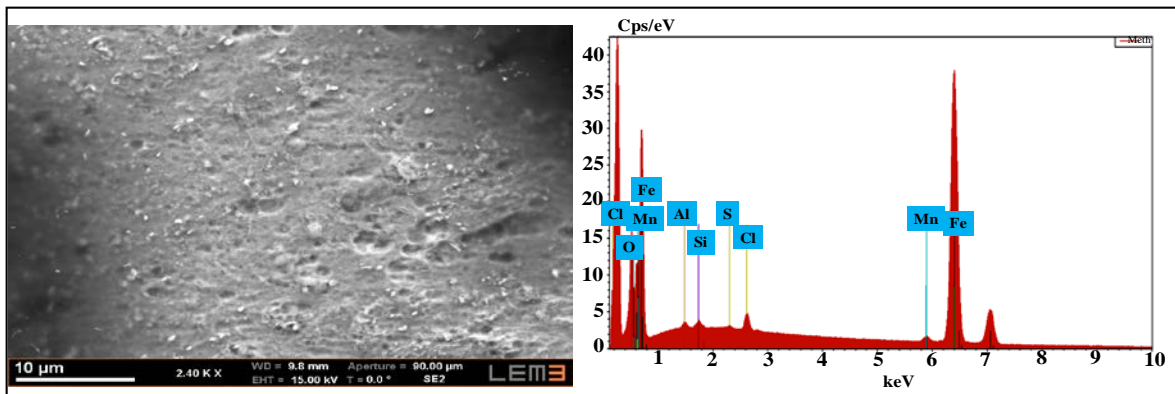

Fig. 13. Top-surface *SEM* image and *EDX* spectrum of the pipeline steel sample in the presence of 0.5 *g/L* of *ME* extract
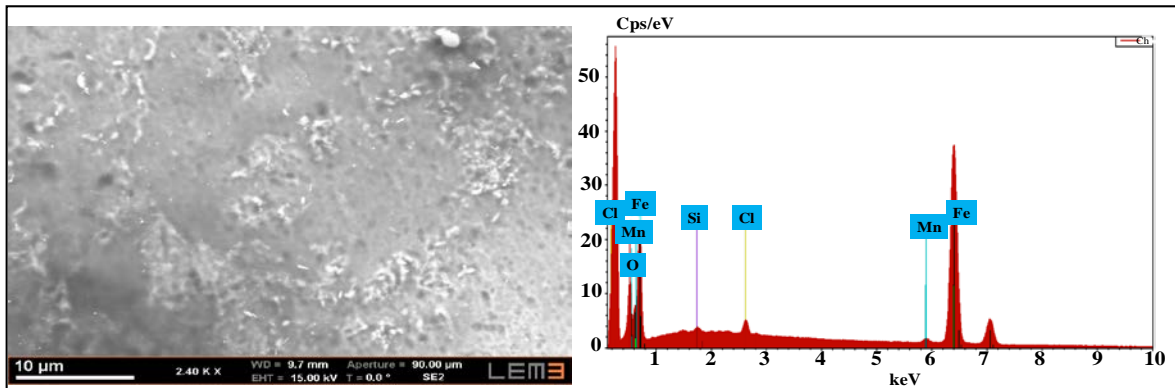

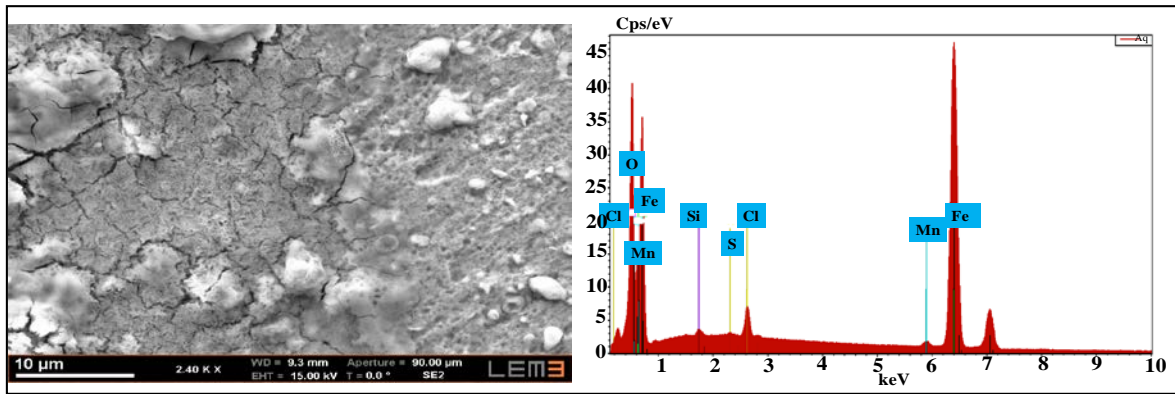**Fig. 14.** Top-surface *SEM* image and *EDX* spectrum of the pipeline steel sample in the presence of 0.5 *g/L* of *CE* extract

Fig. 15. Top-surface *SEM* image and *EDX* spectrum of the pipeline steel sample in the presence of 0.5 *g/L* of *OEAE* extract
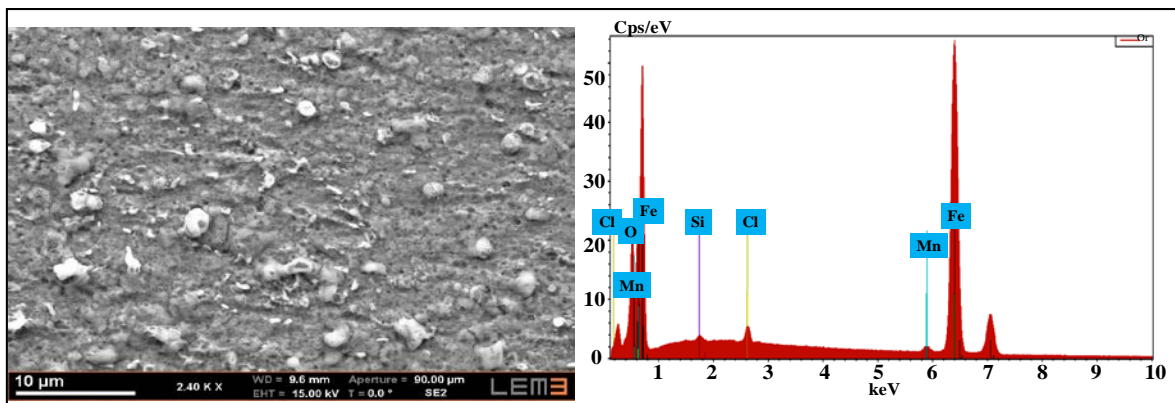

Fig. 16. Top-surface *SEM* image and *EDX* spectrum of the pipeline steel sample in the presence of 0.5 *g/L* of *AEAE* extract
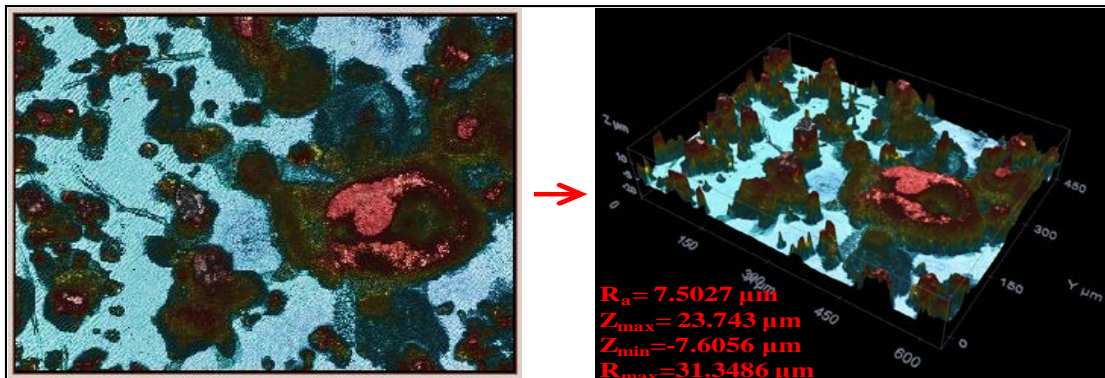

Fig. 17. Three-dimensional optical profiler images of pipeline steel samples after 24 h immersion in *1M HCl*

The *3D* view of the pipeline steel surface exposed to the inhibitor-free corrosive medium (Fig. 17) shows the formation of corrosion pits of various shapes and depths. This corroded surface has also a quite high average roughness (R_a) of 7.50 µm due to the acid attack. The addition of the extracts to the acid medium lead to a decrease in the pitting process intensity (Fig. 18). Besides that, the average roughness of steel surface was also decreased from 7.50 µm for the inhibitor-free experiment to 511.85 nm, 462.43 nm, 1.7313 µm, and 3.9478 µm values for acid solution loaded with the methanol (*ME*), chloroform (*CE*), organic ethyl acetate (*OAEA*) and aqueous ethyl acetate extracts (*AEAE*), respectively. It is worth to note here that the observed reduction in the roughness values with the *CE* and *ME* experiments are in full agreement with the findings results of the electrochemical measurements.

4. Conclusions

We have achieved in this study the successful isolation of various flavonoids extracts from the leaves of *Ruta chalepensis* and their performance as possible corrosion inhibitors for the *API 5L X52* steel in 1M hydrochloric acid solution was carefully investigated. We proved that all the considered extracts have an antioxidant activity, inhibit simultaneously the two oxidation reactions, $Fe \rightarrow Fe^{+2} + 2e^-$ and $Fe^{+2} \rightarrow Fe^{+3} + 1e^-$, and demonstrate a potential ability to inhibit the rust formation ($Fe_2O_3.nH_2O$), i.e. the corrosion process of the given steel.
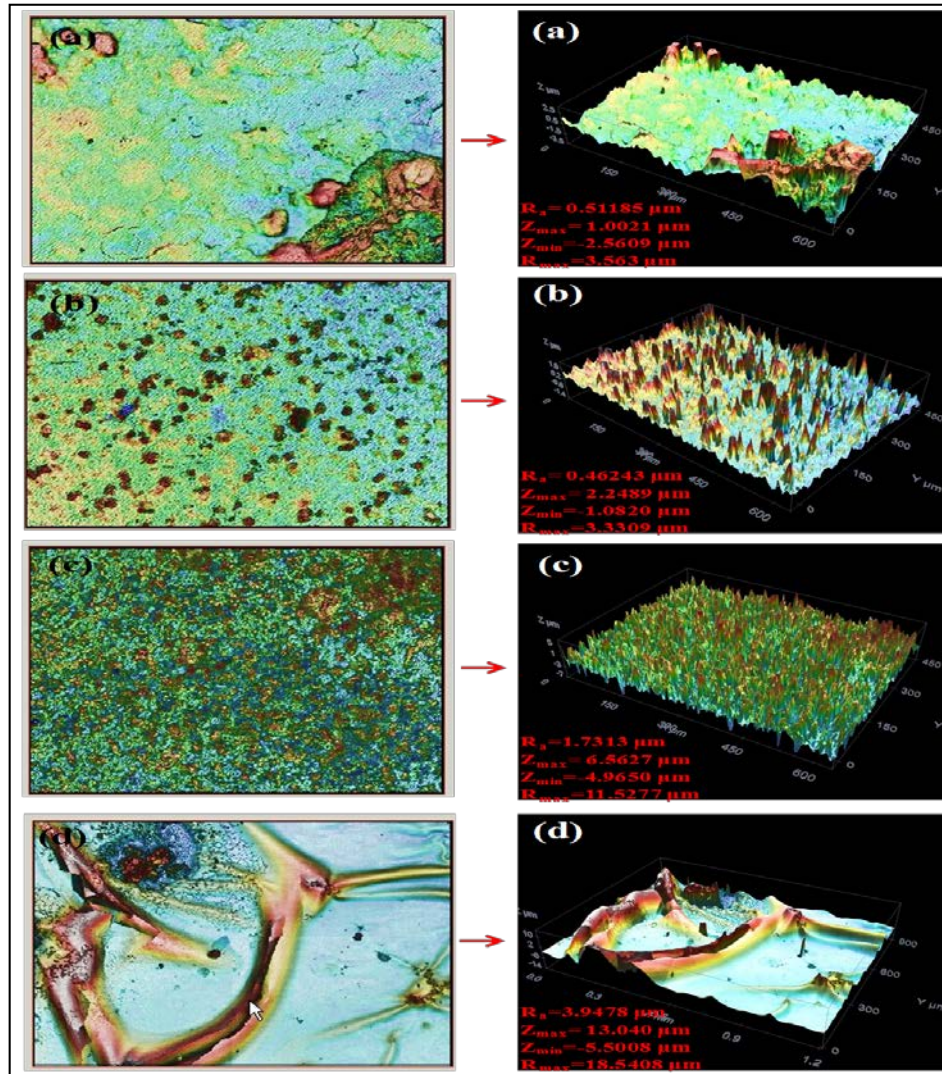
Fig. 18. Three-dimensional optical profiler images of pipeline steel samples in the presence of 0.5 *g/L* of various extracts: (a) *ME*, (b) *CE*, (c) *OEAE* and (d) *AEAE*

The inhibition efficiency of all extracts was in the following order*: CE > ME > OEAE > AEAE*. The abilities of the studied extracts to reduce the corrosion processes were confirmed by the electrochemical measurements and surface analysis results. The chloroform extract (*CE*) can be recommended as a promising corrosion inhibitor for *API 5L X52* steel in acidic media.

References

Abdallah M., Basim H.A., Zaafarany I., Fouda A.S., (2012), The inhibition of carbon steel corrosion in hydrochloric acid solution using some phenolic compounds, *International Journal of Electrochemical Science*, **7**, 282-304.

Akbarirad H., Gohari Ardabili A., Kazemeini S M., Mousavi Khaneghah A., (2016), An overview on some of important sources of natural antioxidants, *International Food Research Journal*, **23**, 928-933.

Bahorun T., Grinier B., Trotin F, Brunet G., Pin T., Luncky M., Vasseur J., Cazin M., Cazin C., Pinkas M., (1996), Oxygen species scavenging activity of phenolic extracts from hawthorn fresh plant organs and pharmaceutical preparations, *Arzneimittel-Forsching*, **46**, 1086-1089.

Benghalia M.A., Fares C., Khadraoui A., Hadj Meliani M., Obot I. B., Sorrour A., Dmytrakhe M., Azari Z., (2018), Performance evaluation of a natural and synthetic compound as corrosion inhibitors of API 5l X52 steel in hydrochloric acid media, *Moroccan Journal of Chemistry*, **6**, 51-61.

Bouledroua O., Hadj Meliani M., Azari Z., Sorour A., Merah N., Pluvinage G., (2017), Effect of sandblasting on tensile properties, hardness and fracture resistance of a line pipe steel used in Algeria for oil transport, *Journal of Failure Analysis and Prevention*, **17**, 890-904.

Brewer M.S., (2011), Natural antioxidants: sources, compounds, mechanisms of action, and potential applications, *Comprehensive Reviews in Food Science and Food Safety*, **10**, 221-247.

Bruneton J., (1993), *Pharmacognosy, Phytochemistry and Medicinal Plants*, (in French), La Voisier TEC et DOC, 2nd Edition, 268-277.

Buchweishaija J., (2009), Phytochemicals as green corrosion inhibitors in various corrosive media: a review, *Tanzania Journal of Science*, **35**, 77-92.

Cotea V.V., Luchian C., Niculaua M., Zamfir C.I., Moraru I., Nechita B.C., Colibaba C., (2018), Evaluation of phenolic compounds content in grape seeds, *Environmental Engineering and Management Journal*, **17**, 795-802.

Cushnie T.P.T., Lamb A.J., (2005), Antimicrobial activity of flavonoids, *International Journal of Antimicrobial Agents*, **26**, 343-356.

Elazzizi A., Hadj Meliani M., Khelil A., Pluvinage G., Matvienko Y.G., (2015), The master failure curve of pipe steels and crack paths in connection with hydrogen embrittlement, *International Journal of Hydrogen Energy*, **40**, 2295-2302.

Farooqi H.I., Quraishi M.A., Saini P.A., (1997), Natural compounds as corrosion inhibitors for mild steel in industrial cooling systems, *Proceedings from European Federation of Corrosion*, **1**, 186-194.

Fouda A.S., Eldesoky A.M., Elmorsi M.A., Fayed T.A., Atia M.F., (2013), New eco-friendly corrosion inhibitors based on phenolic derivatives for protection mild steel corrosion, *International Journal of Electrochemical Science*, **8**, 10219-10238.

Hadj Meliani M., Matvienko Y.G., Pluvinage G., (2011a), Corrosion defect assessment on pipes using limit analysis and notch fracture mechanics, *Engineering Failure Analysis Journal*, **18**, 271-283.

Hadj Meliani M., Matvienko Y.G., Pluvinage G., (2011b), Two-parameter fracture criterion (K,c Tef) based on notch fracture mechanics, *International Journal Fracture*, **167**, 173-182.

Houghton P.J., (1995), The role of plants in traditional medicine and current therapy, *Journal of Alternative and Complementary Medicine*, **1**, 131-134.

Husain S.R., Cillard J., Cillard P., (1987), Hydroxyl radical scavenging activity of flavonoids, *Phytochemistry Journal*, **26**, 2489-2491.

Khadraoui A., Khelifa A., Hadjmeliani M., Mehdaoui R., Hachama K., Tidu A., Azari Z., Obot I.B., Zarrouk A., (2016), Extraction, characterization and anti-corrosion activity of *Mentha pulegium* oil: Weight loss, electrochemical, thermodynamic and surface studies, *Journal of Molecular Liquids*, **216**, 724-731.

Magufuli J.P.J., (2009), *The potential of anacardic acid self-assembled monolayers from cashew nut shell liquid as corrosion protection coatings*, PhD Thesis, University of Dar es Salaam, Tanzania.

Markesbery W.R., Lovell M.A., (1998), Four-hydroxynonenal, a product of lipid peroxidation, is increased in the brain in Alzheimer's disease, *Neurobiology of Aging*, **19**, 33-36.

Markham K.R., (1982), *Technics of Flavonoids Identification*, Academic Press, Michigan University, USA, 1-113.

Medini F., Fellah H., Ksouri R., Abdelly C., (2014), Total phenolic, flavonoid and tannin contents and antioxidant andantimicrobial activities of organic extracts of shoots of the plant Limonium delicatulum, *Journal of Taibah University for Science*, **8**, 216-224.

Mukherjee D., Berchman J., Rajsekkar A., Sundarsanan N., Mahalingam R., Maruthamuthu S., Thiruchelvam T., Karaikudi D., (1997), Plant-based alkaloids inhibit corrosion of marine alloys, *Anti-Corrosion Methods and Materials Journal*, **44**, 186-194.

Mutasingwa J., (2004), *As assessment of cashew nut shell liquid as a corrosion inhibitor of mild steel alloys in flowing aqueous system*, MSc Thesis, University of Dar es Salaam, Tanzania.

Ndibe M., Menkiti M., Ijomah M., Onukwuli D., Ejikeme P., (2018), Acid extract of aloe vera as inhibitor for the corrosion of mild steel in acidic media, *Environmental Engineering and Management Journal*, **17**, 2847-2856.

Obot I.B., Umoren S.A., Gasem Z.M., Suleiman R.K., El-Ali B.M., (2015), Theoretical prediction and electrochemical evaluation of vinylimidazole and allylimidazole as corrosion inhibitors for mild steel in 1M HCl, *Journal of Industrial and Engineering Chemistry*, **21**, 1328-1339.

Okafor P.C., Ebiekpe V.E., Azike C.F., Egbung G.E., Brisibe E. A., Ebenso E.E., (2012), Inhibitory action of artemisia annua extracts and artemisinin on the corrosion of mild steel in H_2SO_4 solution, *International Journal of Corrosion*, **1**, 1-8.

Onuegbu T.U., Umoh E.T., Ehiedu C.N., (2013), *Emilia sonchifolia* extract as green corrosion inhibitor for mild steel in acid medium using weight loss method, *Journal of Natural Sciences*, **3**, 52-55.

Oyaizu M., (1986), Studies on products of browning reaction-Antioxidative activities of products of browning reaction prepared from glucosamine, *Japanese Journal of Nutrition*, **44**, 307–315.

Philip J.N.Y., Buchweishaija J., Mkayula L.L., (2001), Cashew nut shell liquid as an alternative corrosion inhibitor for carbon steel, *Tanzania Journal of Science*, **27**, 9-19.

Pong K., (2003), Oxidative stress in neurodegenerative diseases: therapeutic implications for superoxide dismutase mimetics, *Expert Opinion on Biological Therapy journal*, **3**, 127-139.

Robak J., Gryglewski J., (1988), Flavonoids are scavengers of superoxide anion, *Biochemical Pharmacology Journal*, **37**, 837-841.

Soudani M., Hadj Meliani M., El-Miloudi K., Fares C., Benghalia M.A., (2017), Corrosion effects and green scale inhibitors in the fracture mechanics properties of gas pipelines, *Structural Integrity and Life*, **17**, 25-31.

Takahama U., (1985), Inhibition of lopoxygenase-dpendent lipid peroxidation by quercetin: Mechanism of antioxidative function, *Phytochemistry Journal*, **24**, 1443-1446.

Torel J., Cillard J., Cillard P., (1986), Antioxidant activity of flavonoids and reactivity with peroxy radical, *Phytochemistry Journal*, **25**, 383-385.

Umoren S.A., Solomon M.M., Obot I.B., Suleiman R.K., (2018), Comparative studies on the corrosion inhibition efficacy of ethanolic extracts of date palm leaves and seeds on carbon steel corrosion in 15% HCl solution, *Journal of Adhesion Science and Technology*, **32**, 1934-1951.

Vrsalovic L., Oguzie E., Klissic M., Radosevic J., Gudic S., (2007), Sinapinic acid as Al–2.5Mg alloy corrosion inhibitor in sodium chloride solution, *Journal of Applied Electrochemistry*, **37**, 325-330.

Vrsalovic L., Oguzie E., Klissic M., Gudic S., (2011), Corrosion inhibition of CuNi10Fe alloy with phenolic acids, Chemical Engineering Communications, **198**, 380-393.

Williams R.J., Spencer J.P.E., Rice-Evans C., (2004), Flavonoids: antioxidants or signalling molecules Free radical, *Biology & Medicine*, **36**, 838-849.

Zhang Y.J., Gan R.Y., Li S., Zhou Y., Li A.N., Xu D.P., Li H.B., (2015), Antioxidant phytochemicals for the prevention and treatment of chronic diseases, *Molecules*, **20**, 21138-21156.